

Ergodicity and mixing in quantum theory. II

Mario Feingold

Department of Physics, Technion—Israel Institute of Technology, Haifa 32000, Israel

Nimrod Moiseyev

Department of Chemistry, Technion—Israel Institute of Technology, Haifa 32000, Israel

Asher Peres

Department of Physics, Technion—Israel Institute of Technology, Haifa 32000, Israel

(Received 17 January 1984)

The approach proposed in the first part of this paper is illustrated by two examples. The first one involves the Hénon-Heiles model. A small wave packet, initially localized in the classically chaotic region, evolves so that $\langle x \rangle$ and $\langle x^2 \rangle$ rapidly reach their equilibrium values. The second example makes use of a pair of rotators with nonlinear coupling. The matrix elements of J_z , in the energy representation, are pseudorandom in the energy range which is classically chaotic, but obey selection rules in the classically regular energy range.

In paper I¹ it was suggested that the hallmark of quantum chaos is that simple dynamical variables are represented by pseudorandom matrices when the Hamiltonian is diagonalized. As a consequence, the expectation values of these variables tend to equilibrium values which are insensitive to the initial state preparation, for nearly all preparations involving many energy levels. We shall now illustrate this approach by investigating the quantum behavior of two physical systems which are classically chaotic in some regions of phase space and regular in others.

I. HÉNON-HEILES WAVE PACKET

The Hénon-Heiles oscillator is defined by the Hamiltonian²

$$H = \frac{1}{2}(p_x^2 + p_y^2 + x^2 + y^2) + x^2y - \frac{1}{3}y^3. \quad (1)$$

Its classical behavior is well documented.^{3,4} In some regions of phase space most orbits are regular, in others most are chaotic, and there are also some regions with mixed behavior.

The time evolution of a small wave packet, in the quantized version, was recently investigated by two of us.⁵ A wave packet initially located in a regular region of the classical phase space follows the classical trajectory and spreads very slowly. On the other hand, a wave packet initially located in chaotic region spreads very rapidly. This may perhaps be considered as a trivial consequence of the classical limit of Schrödinger's equation.⁶ However, it is *not* trivial that the second wave packet, when observed on a coarse scale, also tends to an *equilibrium* configuration. Figure 1 shows the behavior of $\langle x \rangle$ and $\langle x^2 \rangle$ for the wave packet initially given by

$$\psi = (\pi\hbar)^{-1/2} \exp \left[-\frac{x^2}{2\hbar} + \frac{i\dot{x}_0 x}{\hbar} - \frac{(y-y_0)^2}{2\hbar} \right], \quad (2)$$

with $\dot{x}_0 = 0.459757$ and $y_0 = -0.185405$ (this is a hyper-

bolic fixed point in the chaotic region of phase space, corresponding to an unstable periodic orbit, with energy 0.125 and period $\tau = 6.90853$).⁴ We see from Fig. 1 that after a few periods $\langle x \rangle$ and $\langle x^2 \rangle$ are very close to their equilibrium values 0 and ~ 0.095 , respectively. The tendency of such wave packets to "settle" around equilibrium values was also noted by other authors.⁷

In these calculations⁵ we took $\hbar = 0.015$ and used 324 basis functions. The Hamiltonian matrix had to be truncated (because of computer limitations). Relatively few (about 50) energy levels were appreciably populated.⁵ Thus, if Fig. 1 were extended for longer times, it would soon display fluctuations of $\langle x \rangle$ and $\langle x^2 \rangle$, possibly large ones. It may be objected that this truncation of the Hamiltonian alters the nature of the Hénon-Heiles system and impairs the correspondence between its classical and quantized versions. The dynamical model discussed in Sec. II overcomes these difficulties.

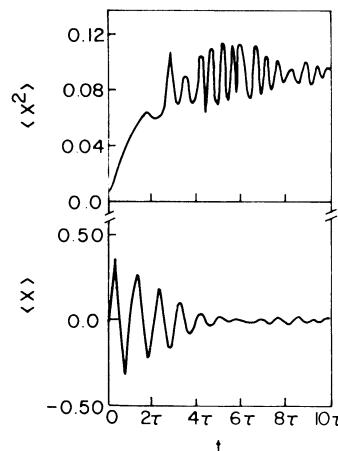


FIG. 1. The chaotic wave packet initially given by Eq. (2) reaches equilibrium after only a few oscillations. The classical period is $\tau = 6.90853$.

II. NONLINEARLY COUPLED ROTATORS

We consider two “rotators,” namely, physical systems having the same commutation relations as angular momenta \vec{L} and \vec{M} ,

$$[L_x, L_y] = i\hbar L_z, \quad (3a)$$

$$[M_x, M_y] = i\hbar M_z, \quad (3b)$$

and cyclic permutations, and

$$[L_i, M_j] = 0, \quad (3c)$$

for all i and j .

The Hamiltonian in this model is taken as⁸

$$H = L_z + M_z + L_x M_x. \quad (4)$$

(There is no physical system with such a Hamiltonian, but it is somewhat similar to those used with quasispins in nuclear physics⁹ or pseudospins in solid state physics.¹⁰) It will be convenient to define

$$J_z = L_z + M_z. \quad (5)$$

The “classical” constants of motion (those which are well behaved in the limit $\hbar \rightarrow 0$) are H , L^2 , and M^2 . There is also one modular¹¹ (nonclassical) constant of motion which can be written as $J_z \pmod{2\hbar}$ or $\cos(\pi J_z / \hbar)$, etc., because the $L_x M_x$ term in (4) has selection rules $\Delta J_z = 0, \pm 2\hbar$.

The classical system with Hamiltonian (4) and Poisson brackets in lieu of commutators has both regular and chaotic orbits,⁸ just like the Hénon-Heiles oscillator. Figure 2 shows the regions of phase space where we found only regular orbits, only chaotic ones, or orbits of both types in the special case $L = M$. The energy scale in Fig. 2 has been normalized by dividing the energy E by its maximum classical value⁸

$$E_{\max} = \begin{cases} 2L & \text{if } L < 1, \\ 1 + L^2 & \text{if } L > 1. \end{cases} \quad (6a)$$

$$(6b)$$

While the values of L^2 and M^2 are arbitrary in classical physics, their quantum counterparts must satisfy

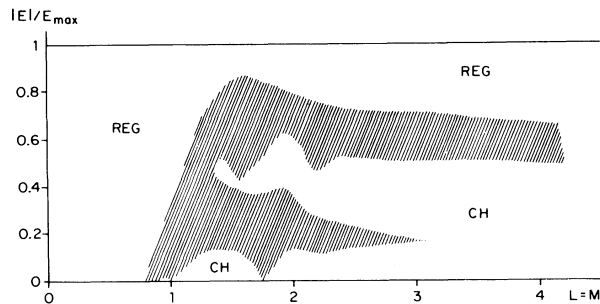


FIG. 2. The regular and chaotic domains of the Hamiltonian (4) when the constants of motion L^2 and M^2 are equal. In the hatched region we found both regular and chaotic orbits. As shown in Ref. 8, the figure is symmetric with respect to the sign of the energy E . The maximum classical value of $|E|$ for given $L = M$ is given by Eq. (6).

$L^2 = \hbar^2 l(l+1)$ and $M^2 = \hbar^2 m(m+1)$, where l and m are integers or half integers. As these are constants of the motion, the Hamiltonian matrix is reducible (block diagonal), each block being labeled by the values of l and m . In other words, for given l and m , the Hamiltonian is a matrix of finite order. There is no need of truncation.

Naturally, we cannot have true chaos in a finite dimensional Hilbert space. We can nevertheless inquire how these matrices behave in the semiclassical limit $\hbar \rightarrow 0$, when the values of L and M are kept finite, so that l and m become very large. We thus write $\vec{L} = \hbar \vec{l}$ and $\vec{M} = \hbar \vec{m}$, where \vec{l} and \vec{m} are standard numerical matrices¹² of order $2l+1$ and $2m+1$, respectively. The Hamiltonian H requires a direct product of these matrices¹² and is therefore represented by a matrix of order $(2l+1)(2m+1)$.

Our first task is to find the eigenvalues and eigenvectors of H . It is convenient to take a representation where l_z and m_z are diagonal. Note that the maximum value of $j_z = l_z + m_z$ is $l+m$. We can therefore study separately the two subspaces where $l+m-j_z$ is odd or even because of the selection rule mentioned above. Moreover, in the special case $l=m$, a further reduction is possible. The Hamiltonian is conspicuously invariant under the interchange of \vec{L} and \vec{M} and, therefore, if $l=m$, its eigenfunctions $\psi(m, m, l_z, m_z)$ must be either odd or even with respect to the interchange of l_z and m_z . No further reduction of the Hamiltonian matrix is possible (for lack of a better proof we note that such a reduction would have been immediately detected in the calculations discussed below).

The properties of the energy eigenvalues have been discussed elsewhere.¹³ As expected from the correspondence principle, the quantum energy levels are arranged in nearly equidistant sets in the regular region of the classical phase (say, for $L=M < 0.8$). There is no such regular spacing in the chaotic region.¹⁴ However, for finite \hbar quantum chaos is more remote than classical chaos. This can be explained by the existence of tori remnants.^{15,16} As long as the missing parts of these “vague tori” are small compared to $2\pi\hbar$, the quantum system behaves as if it were regular, with nearly equidistant sets of energy levels, selection rules, etc.

As an example we examined the case $L=M=3.5$. We then have from Eq. (6), $E_{\max} = 13.25$ and we see from Fig. 2 that classical orbits are mostly regular for $|E| \gtrsim 9.1$ and mostly chaotic for $|E| \lesssim 6.6$. From the general arguments of paper I¹ we thus expect that when a “reasonable” operator such as J_z is represented in the energy basis, it will have “random” matrix elements $(J_z)_{E'E''}$ when $|E'|$ and $|E''| \lesssim 6.6$ and “regular” (mostly zero) matrix elements when $|E'|$ and $|E''| \gtrsim 9.1$. These figures are actually valid only in the semiclassical limit $\hbar \rightarrow 0$. For finite \hbar the regular domain is larger and the chaotic domain smaller because of the vague tori.

The reader should note that what we propose here is to consider two submatrices of the same matrix (i.e., the same operator of the same physical system, with the same Hamiltonian, the same value of \hbar , etc., but in different parts of the energy spectrum, corresponding to different regions of the classical phase space). This choice is necessary in order to obtain an unbiased comparison between

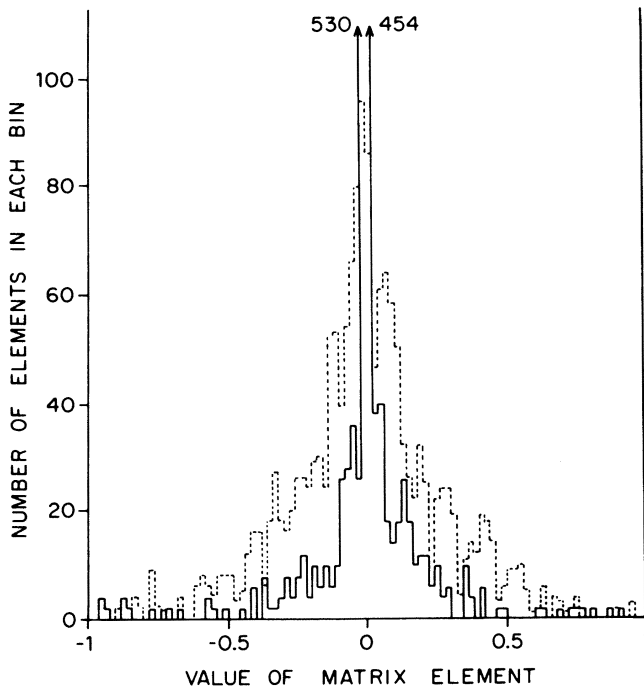


FIG. 3. Histograms for the values of the matrix elements $(J_z)_{E'E''}$ in two 40×40 submatrices: $E', E'' > 6.98$ (solid line) and $0 < E', E'' < 1.24$ (broken line). The first submatrix, which corresponds to the regular part of the spectrum, has most of its elements very close to zero. On the other hand, the elements of the second submatrix, which corresponds to the chaotic part of the spectrum, have a roughly Gaussian distribution. Not shown on these histograms are 94 elements of the first submatrix and 5 elements of the second one whose absolute values exceed 1 (see text).

“chaotic” and “regular” matrix elements.

We have performed the calculations by taking $l=m=20$ (this corresponds to $\hbar=0.1707825$ to make $L=M=3.5$). We considered only the “even-even” subspace of the Hamiltonian, i.e., eigenfunctions $\psi(20, 20, l_z, m_z)$ with even $j_z = l_z + m_z$ and which are invariant under $l_z \leftrightarrow m_z$. This subspace has dimension

$(l+1)^2=441$. We diagonalized H and found its eigenfunctions. It turned out, as expected, that most energy levels were regular (i.e., arranged in nearly equidistant sets) down to about $|E| \simeq 6.8$. This roughly corresponds to the middle of the transition region in Fig. 2 less $2\pi\hbar$. Of course there is no sharp “phase transition” in the spectrum, but a *gradual* change from regularity to chaos.

We computed the matrix elements $(J_z)_{E'E''}$.¹⁷ We then examined *three* 40×40 submatrices of J_z : one with the 40 highest eigenvalues of E' and E'' (namely, $E', E'' > 6.98$, in the regular region), one with $0 < E', E'' < 1.24$ (in the chaotic region), and one off-diagonal submatrix, with E' in the regular region and E'' in the chaotic region.

The 1600 elements of the first two submatrices of J_z were placed in bins of width 0.02. The result is shown in Fig. 3. As expected, most elements of the regular submatrix are very close to zero, while most of those of the chaotic submatrix are not. Their distribution appears roughly Gaussian. The histograms of Fig. 3 were truncated, for lack of space, at -1 and 1 . The regular submatrix also had 62 elements between 1 and 3.27, and 32 elements between -2.01 and -1 . The chaotic submatrix had only 5 elements between 1 and 1.18 and no element below -1 .

The off-diagonal submatrix (E' regular, E'' chaotic) had *all* its elements very small. Only 51 of them exceeded (in absolute value) 10^{-6} ; none exceeded 10^{-5} . This result was expected because regular and chaotic wave functions do not overlap. They “exist” mostly in the regular and chaotic regions of classical phase space, respectively.¹⁸

Similar results hold in the other invariant subspaces of the Hamiltonian and for other “simple” operators such as L_x or M_y , etc., or powers thereof. In summary, our definition of quantum chaos¹ (simple dynamical variables are represented by pseudorandom matrices when H is diagonal) appears unambiguously satisfied in the model of nonlinearly coupled rotators.

ACKNOWLEDGMENTS

Part of this paper (Sec. II) is based on the thesis by one of us (M.F.). This research was supported by the U.S.-Israel Binational Science Foundation and the Gerard Swope Fund.

¹A. Peres, preceding paper [Phys. Rev. **30**, 504 (1984)].

²M. Hénon and C. Heiles, Astron. J. **69**, 73 (1964).

³G. Walker and J. Ford, Phys. Rev. **188**, 416 (1969).

⁴S. J. Feingold and A. Peres, Phys. Rev. A **26**, 2368 (1982).

⁵N. Moiseyev and A. Peres, J. Chem. Phys. **79**, 5945 (1983).

⁶E. Madelung, Z. Phys. **40**, 322 (1926).

⁷J. S. Hutchinson and R. E. Wyatt, Phys. Rev. A **23**, 1567 (1981).

⁸M. Feingold and A. Peres, Phys. D **9**, 433 (1983).

⁹R. D. Williams and S. E. Koonin, Nucl. Phys. **A391**, 72 (1982) and references therein.

¹⁰C. Buzano, M. Rasetti, and M. Vadamchino, Prog. Theor. Phys. **68**, 703 (1982).

¹¹Y. Aharonov, H. Pendleton, and A. Petersen, Int. J. Theor. Phys. **2**, 213 (1969).

¹²J. L. Powell and B. Crasemann, *Quantum Mechanics* (Addison-Wesley, Reading, Mass., 1961), pp. 344–366.

¹³A. Peres, in *Quantum Chaos*, edited by G. Casati and J. Ford (Academic, New York, 1984).

¹⁴P. Pechukas, Phys. Rev. Lett. **51**, 943 (1983).

¹⁵C. Jaffé and W. P. Reinhardt, J. Chem. Phys. **77**, 5191 (1982).

¹⁶R. B. Shirts and W. P. Reinhardt, J. Chem. Phys. **77**, 5204 (1982).

¹⁷The matrix elements are real, with the customary choice of phases. We started with real symmetric matrices for J_x and J_z , and therefore for H . We then took all the eigenvectors of H as real. This ensures that J_x and J_z remain real symmetric and J_y is imaginary and antisymmetric.

¹⁸M. V. Berry, Phil. Trans. R. Soc. London, Ser. A **287**, 237 (1977).